Title: *ESR1* F404 mutations and acquired resistance to fulvestrant in *ESR1* mutant breast cancer.

Authors and affiliations:

Belinda Kingston[1], Alex Pearson[1], Maria Teresa Herrera-Abreu[1], Li-Xuan Sim[1], Rosalind J Cutts[1], Heena Shah[1], Laura Moretti[2], Lucy S Kilburn[2], Hannah Johnson[2], Iain R Macpherson[3], Alistair Ring[4], Judith M Bliss[2], Yingwei Hou [5], Weiyi Toy[6], John A Katzenellenbogen[5], Sarat Chandarlapaty[6], Nicholas C Turner[1,4]

[1] The Breast Cancer Now Toby Robins Research Centre, The Institute of Cancer Research, London, SW3 6JB.

[2] Clinical Trials and Statistics Unit at The Institute of Cancer Research, London, UK

[3] School of Cancer Sciences, University of Glasgow, Glasgow, G61 1QH

[4] Breast Unit, The Royal Marsden Hospital, Fulham Road, London.

[5] Department of Chemistry and Cancer Center at Illinois, University of Illinois at Urbana-Champaign, Urbana, Illinois.

[6] Memorial Sloan Kettering Cancer Center, New York City; Department of Medicine, Weill Cornell Medical College, New York City, USA.

Running title:

Mutations of *ESR1* at F404 confer fulvestrant resistance.

Keywords:

Fulvestrant, acquired resistance, breast cancer.

Additional information.

BK is supported by Cancer Research UK Grant A25161 and Institutional funding from Breast Cancer Now. AP, MTHA, LXS and NCT are supported by funding from Breast Cancer Now. Research support for J.A.K. and Y.H. was provided by the National Institutes of Health (NIH/NCI, 1R01 CA220284) and the Breast Cancer Research Foundation (BCRF-084). SC is supported by NIH Cancer Center Support Grant P30-CA008748 and NIH R01CA245069.

Corresponding author:

Prof Nicholas Turner, The Breast Cancer Now Toby Robins Research Centre, The Institute of Cancer Research, London, SW3 6JB. nick.turner@icr.ac.uk 020 7811 8914/ext4737.

Conflict of interest disclosure statement:

BK has received a grant from Cancer Research UK, and honoraria from Guardant Health outside the submitted work. AR has received honoraria for advisory boards and talks: Novartis, Astra Zeneca, Daiichi-Sankyo, Roche, Pfizer, Lilly, Gilead, MSD, Seagen, Stemline. IRM has paid consultancy for Roche, Novartis, Pfizer, Eli Lilly, Pierre Fabre, Daiichi Sankyo, and AstraZeneca, and received travel/conference expenses from Roche, Eli Lilly, and Daiichi Sankyo. SC has received research grant support from Daiichi-Sankyo, AstraZeneca, and Ambrx; financial interests in Totus Medicines and Odyssey Biosciences; and consulting fees from Novartis, AstraZeneca, Lilly, and Paige.ai. NT has received advisory board honoraria from Astra Zeneca, Bristol-Myers Squibb, Lilly, Merck Sharpe and Dohme, Novartis, Pfizer, Roche/Genentech, GlaxoSmithKline, Zentalis pharmaceuticals, Repare therapeutics, Arvinas, Inivata and research funding from Astra Zeneca, BioRad,

Pfizer, Roche/Genentech, Merck Sharpe and Dohme, Guardant Health, Invitae, Inivata, Personalis, Natera. AP, MTHA, LXS, RC, HS, LM, LK, HJ, JB, YH, YW, and JAK declare no conflict of interest.

Word count: 4988, including 6 figures and 1 table.

Abstract

Fulvestrant is used to treat patients with hormone receptor positive advanced breast cancer but acquired resistance is poorly understood. PlasmaMATCH Cohort A (NCT03182634) investigated the activity of fulvestrant in patients with activating *ESR1* mutations in circulating tumor DNA (ctDNA). Baseline *ESR1* mutations Y537S associated with poor, and Y537C with good outcome. Sequencing of baseline and EOT ctDNA samples (n=69) revealed 3/69 (4%) patients acquired novel *ESR1* F404 mutations (F404L, F404I, F404V), in *cis* with activating mutations. *In silico* modelling revealed that *ESR1* F404 contributes to fulvestrant binding to ERα through a *pi*-stacking bond, with mutations disrupting this bond. *In vitro* analysis demonstrated that single F404L, E380Q, and D538G models were less sensitive to fulvestrant, while compound mutations D538G+F404L and E380Q+F404L were resistant. Several oral ERα degraders were active against compound mutant models. We have identified a resistance mechanism specific to fulvestrant, that can be targeted by treatments in clinical development.

Statement of significance

Novel F404 *ESR1* mutations may be acquired to cause overt resistance to fulvestrant when combined with pre-existing activating *ESR1* mutations. Novel combinations of mutations in the ER ligand binding domain may cause drug-specific resistance, emphasising the potential of similar drug-specific mutations to impact efficacy of oral ER degraders in development.

Introduction

For estrogen receptor positive (ER+) breast cancer, which accounts for 75% of breast cancers, hormonal therapy forms the backbone of treatment. In advanced breast cancer (ABC), the selective estrogen receptor degrader (SERD) fulvestrant is licenced for use in the first and second line, both as a single agent, and in combination with targeted therapies including CDK4/6 inhibitors and alpelisib(1-3). Fulvestrant acts by competitively inhibiting the binding of estradiol to ERα(4), impeding receptor dimerization and nuclear localisation(5,6), preventing the activation of estrogen response elements within the regulatory regions of estrogen sensitive genes. Fulvestrant-bound ER is also unstable, leading to increased degradation of the estrogen receptor(6). Although a standard therapy for patients with ABC, few studies have investigated mechanisms of resistance to fulvestrant.

Activating estrogen receptor mutations (*ESR1* mutations) are acquired through prior aromatase inhibitor therapy for ABC(7), with circulating tumour DNA analysis demonstrating that the mutations are present in 15-40% of patients treated with prior aromatase inhibition(8-10). Activating *ESR1* mutations, that cluster at specific amino acids in the ligand binding domain (LBD), result in ligand independent activation of *ESR1*. Fulvestrant binding to mutant ERα is partially impaired, with higher concentrations of fulvestrant required to inhibit mutant ERα *in vitro*(5,11). It is considered unlikely that fulvestrant achieves concentrations required to optimally inhibit mutant *ESR1* in the clinic, and new oral SERDS that do fully inhibit *ESR1*, such as elacestrant, have improved activity as single agents(12-14).

The plasmaMATCH trial investigated the activity of a range of targeted treatments in patients selected based on plasma circulating tumour DNA (ctDNA) testing. Cohort A

enrolled patients with ER+ ABC with activating *ESR1* mutations for treatment with fulvestrant. Prior clinical research suggests a fulvestrant dose response (15,16), and patients were treated with extended dose fulvestrant (500mg) given every 2 weeks, twice as frequent as standard dosing, to increase fulvestrant exposure and target *ESR1* mutant cancers. Median progression free survival was 2.2 months (17). Here we investigate the genomic associations of response and resistance to fulvestrant in Cohort A of the plasmaMATCH trial. We demonstrate that baseline *ESR1* variants are predictive of response to fulvestrant, with frequent acquisition of potentially targetable mutations. We identify mutations at F404 in estrogen receptor, that occur in *cis* with classical activating *ESR1* mutations, and are acquired as a mechanism of resistance to fulvestrant, identifying the first mechanism of acquired resistance specific to fulvestrant.

Results

Baseline *ESR1* variants and differential fulvestrant activity

Of the 84 patients enrolled onto Cohort A treated with extended dose fulvestrant, 79 (94%) had targeted sequencing results available for analysis, all of whom had detectable ctDNA. The observed baseline mutations reflected the profile of aromatase inhibitor pre-treated advanced breast cancer. Mutations in *ESR1* (96%, 76/79 patients), *PIK3CA* (43% 34/79 patients) and *TP53* (30% 24/79 patients) were the most commonly identified at baseline (Figure 1A). Median PFS in patients with neither *PIK3CA* nor *TP53* mutations was not significantly altered (Supplementary Figure 1A and B). The most frequent activating *ESR1* alterations in the Cohort were D538G (n = 44, 55.7%), Y537S (n = 34, 43.0%), E380Q (n = 22, 27.9%), Y537N (n = 22, 27.9%), Y537C (n = 11, 13.9%), L536R (n = 7, 8.9%) and S463P (n = 4, 5.1%; Figure 1B). We assessed the impact baseline *ESR1* mutations had on fulvestrant efficacy. Patients with detectable baseline Y537C alterations had longer median progression-free survival (PFS) on fulvestrant compared to patients with other baseline *ESR1* mutations (5.6 month detected versus 2.0 months not detected, HR 2.8 [95% CI 1.3 to 5.9]; Figure 1C *left* panel). Conversely, patients with a baseline Y537S mutation had shorter median PFS (1.8 detected versus 3.5 months not-detected, HR 0.53 (95% CI 0.33 to 0.86; Figure 1C *right* panel). Median PFS in patients on fulvestrant with a baseline D538G, E380Q, and Y537N mutations was not significantly different compared to patients with other baseline *ESR1* mutations (Supplementary Figure 1C-E). To assess the impact of common activating mutations on fulvestrant activity *in vitro*, we conducted a screen of MCF7 cells with transient transfection of mutant *ESR1* expression constructs, assessing the impact of mutations on fulvestrant activity on an ERE reporter construct. Matching the clinical

observations, Y537S induced a high level of resistance to fulvestrant, whilst Y537C was more sensitive (Figure 1D). This provides further evidence for fulvestrant resistance of Y537S mutations, adding to the prior data *in vitro* and *in vivo* (11,18-20), and clinical trial data (21).

Acquired mutations on fulvestrant.

Progression plasma DNA was sequenced in 70 patients, of whom 69 had a baseline plasma sequenced (69/84, 82% enrolled patients). Pathogenic alterations were acquired in 51% patients (35/69), particularly within estrogen and PI3K/AKT signalling pathways (Figure 2A and Supplementary Figure 1F), including 17/69 (25%) patients who acquired potentially targetable alterations, in genes including *PTEN, BRCA1/2, PIK3CA, HER2* and *BRAF* (Figure 2A). The total number of acquired alterations was not different in patients who gained clinical benefit (PR/SD >=24 weeks) versus those that did not (Supplementary Figure 1G). For *ESR1* mutations, the majority of patients (n = 50, 72.5%) maintained their respective poly- or monoclonal *ESR1* mutations, with 5.8% (n = 4) acquiring polyclonal disease through the course of treatment. In all 14/69 (20%) patients acquired *ESR1* mutations at progression, including with 6/69 (9%) patients who acquired L536 mutations. This matched the result of our *ESR1* activation mutation ERE screen, in which L536 mutations were the most resistant to fulvestrant (Figure 1D), likely suggesting that L536 clones were selected through treatment due to fulvestrant resistance.

Identification and investigation of *ESR1* F404, a novel acquired mutation.

We noted that 3/69 (4%) patients acquired mutations at F404 on progression (Figure 2B), a mutation that had not previously been described amongst *ESR1* mutations, including one patient with five separate F404 mutations. The F404 locus is situated

within the LBD of *ESR1,* with codon TTT encoding the phenylalanine (Figure 2C). All three patients had either a partial response or stable disease as their best response on fulvestrant. Of the patients with PFS ≥16 weeks, 12% acquired F404 mutations. We additionally identified H356Y mutations in 3/69 (4%) patients, all in patients with an activating L536P mutation, although subsequent functional experiments suggested H356Y mutation did not impact ERα function (Supplementary Figure 2A and 2B).

All 3 of the patients with acquired F404 mutations harboured activating *ESR1* E380Q mutations at baseline, whilst two of the patients also had baseline D538G mutations. *Cis/trans* analysis of the three patients with co-mutant E380Q (a loci close enough to F404 to be able to establish *cis/trans* patterns in ctDNA) revealed that 6/7 F404 base changes detected in these patients occurred in *cis* with the E380Q mutation (Figure 2D; Supplementary Figure 3). The patient with the mutation in *trans* with E380Q had additional *ESR1* mutations (D538G, S463P and Y537N), and it is possible that the F404 mutation was in *cis* with one of those mutations.

In the absence of prior fulvestrant exposure F404 mutations were very rare. Only 1/800 (0.1%) screening plasma samples from the plasmaMATCH study had an F404 mutation, and this one patient had previously received fulvestrant and had activating mutations in *ESR1* at D538G, E380Q, S463P and Y537N. Furthermore, we interrogated other ctDNA data sets. In the PIPA combination study of fulvestrant, palbociclib and taselisib, 1/16 (6%) patients acquired an F404 mutation at progression (22). In the SERENA-1 study of the novel SERD camizestrant, baseline F404 mutations were identified in 2/214 (1%) patients both of whom had had prior fulvestrant exposure and had other activating *ESR1* mutations(23). Therefore, F404 mutations were found only with prior fulvestrant exposure, only in combination with

other classical activating *ESR1* mutations, and occurred in *cis* with activating mutations expected to result in a translated protein that would carry the compound amino acid changes.

The F404 amino acid residue contains an aromatic ring that, when estrogen is bound to the receptor, forms a *pi*-stacking bond with a corresponding aromatic ring within estrogen. Within the patients who harboured a F404 alteration, all base changes lead to substitution of phenylalanine with one of either isoleucine, valine, or leucine, all of which lack an aromatic ring (Figure 2E). Fulvestrant has a similar structure to estrogen and includes an aromatic ring that forms a *pi*-staking bond with F404 in structural modelling (Figure 2F). *In silico* analysis of binding energies (Supplementary Methods), on mutant *ESR1* backgrounds (*Y537S or L536S)*, suggested mutations at F404 reduced the binding affinity of estrogen and fulvestrant to the estrogen receptor (Supplementary Table 1). This potentially explains the clinical observation that F404 mutations only occurred in the presence of other activating *ESR1* mutations, as F404 mutation might otherwise impair estrogen binding and receptor activation in a wild-type ERα receptor.

Generation and validation of *ESR1* F404L models

We investigated the functional consequences of F404 alteration, and the potential role in fulvestrant resistance, using both CRISPR knock in models and transfection of expression constructs. For both approaches, *ESR1* 1210T>C (F404L), one of the most frequently identified F404 variants, was modelled as a single mutation (F404L) or as a compound mutation in *cis* alongside activating *ESR1* mutations, D538G (1613A>G) and E380Q (1138G>C) selected for investigation as the most frequently co-occurring mutations in the clinical dataset.

MCF7 cells were subjected to CRISPR-Cas9 with homology directed repair (HDR) to "Knock In" the target mutations. Clones were screened by Sanger sequencing of genomic DNA. Any clones identified to harbour the targeted mutations were expanded and expression of the mutant transcript confirmed by RT-PCR and Sanger sequencing (Figure 3A). 3/72 (4%) F404 clones harboured the mutation, of which only 1/3 (33%; F404L_D10) was found to express F404L. 3/59 (5%) D538G clones harboured the mutation, all which 3/3 (100%) expressed the mutant protein. One of D538G clones, D538G_D6C was noted to be homozygous for the mutation providing an ideal background into which to knock in the p.F404L (Figure 3A). A second round of CRISPR was used to introduce F404L into the D538G_D6C model, with cells divided into pools and subjected to estrogen free conditions without (E) and with (EF) fulvestrant (0.5μM). 4/24 (17%) clones selected in the absence of estrogen (E) had expression of F404L (Figure 3A). In contrast, 28/30 (93%) of clones selected with fulvestrant (EF) had expression of F404L, providing clear evidence of preferential selection.

Growth of both the parental MCF7 and F404L_D10 cells was estrogen dependent. In contrast, all models expressing D538G, and compound D538G+F404L, exhibited estrogen independent growth (Figure 3B and 3C). Similarly, D538G expressing models showed estradiol independent expression of the estrogen target gene progesterone receptor (PgR) and trefoil factor1 (TFF1; Figure 3D), whereas F404L showed estradiol dependent expression. Using an ERE-luciferase reporter gene construct and transient expression, we further assessed the impact of F404L and compound F404L+D538G mutations on estrogen mediated signalling (Figure 3E). Cells transfected with D538G tended to increase ERE activity in the absence of estrogen compared to cells expressing wild type *ESR1* (Figure 3F). Notably, cells

expressing F404L showed lower ERE activity compared to cells expressing wild type *ESR1* when exposed to estrogen (P=0.0488, n=4; Figure 3F). Similarly, the combination of E380Q, a less potent activator of ER signalling than D538G, and F404L reduced ERE activity compared to wild type *ESR1* (P<0.023, n=4). Together these results are consistent with the hypothesis that F404L impacts the LBD of ERα, without activating the receptor.

Compound F404 mutations and resistance to fulvestrant

We explored the impact of F404L on sensitivity of MCF7 cells to fulvestrant. CRISPR models expressing F404L had modestly reduced in sensitivity to fulvestrant compared to parental MCF7 cells in both short- and long-term assays (Figure 4A, 4B and 4C). Resistance to fulvestrant was substantially more marked in compound D538G+F404L models showing profound resistance (Figure 4A and 4B). Similarly, quantification of long-term colony formation assays show the compound D538G+F404L models clear resistance to fulvestrant (Figure 4C). Single mutant CRISPR F404L, D538G models and parental MCF7 cells had decreased expression of PgR, TFF1 and ERα when treated with fulvestrant (Figure 4D). In contrast, models with compound D538G+F404L had limited changes in expression of PgR, TFF1 and ERα when treated with fulvestrant (Figure 4D). Supporting these observations, ERE activity associated with transient expression of single and compound *ESR1* variants was reduced by treatment with fulvestrant, with the exception of D538G+F404L which maintained ERE activity compared to cells treated with estradiol alone (Figure 4E). Consistent with this, the combination of F404L+L536P, a combination not seen in the clinical dataset, maintained ERE activity when treated with fulvestrant (Supplementary Figure 3). Together this data confirms that the combined effect of

compound F404 and activating *ESR1* mutations in *cis* in the same protein caused profound fulvestrant resistance.

Compound F404 mutations increase estrogen dependent gene expression.

To extend the observations of increased estrogen signalling in F404 compound models treated with fulvestrant (Figures 3C and 4C), RNAseq was performed for models grown in estradiol (1nM) with and without fulvestrant (1μM) for 24 hours (n=3). Gene set enrichment analysis (GSEA) of D538G+F404L compound mutant models grown with estrogen had decreased “Early estrogen pathway” expression but were otherwise similar to D538G mutant cells (Figure 5A, FDR adjusted q<0.05;). However, when treated with fulvestrant for 24hr, E2F transcription, MYC, proliferation and estrogen mediated signalling were all significantly increased in the compound mutant model (Figure 5B, FDR adjusted q<0.05;). The F404L-D10 model had significant upregulation of estrogen signalling compared to the wildtype control (FDR adjusted q<0.05). Similarly, estrogen signalling was increased in the D538G-D6C model compared to the wildtype control maintained with and without fulvestrant treatment (FDR adjusted q<0.05; Figure 5C). Addition of F404L to D538G (D358G+F404L_EF models), showed significant activation of both E2F target and estrogen response (early and late) pathways with fulvestrant treatment (FDR adjusted q<0.05; Figure 5C). Differential response of the late estrogen response genes illustrated in Figures 5D (estradiol; Supplementary Figure 4A) and 5E (Fulvestrant; Supplementary Figure 4B).

We noted two observations that suggested *ESR1* F404 mutations might be deleterious in the absence of fulvestrant. F404 Compound mutations had lower “Early estrogen pathway” expression (Figure 5A), and introduction of F404 reduced

ERE activity compared to wildtype protein in the presence of estrogen (Figure 3E). Consistent with this the three double mutants expressing F404L models that were selected in the presence of estrogen “E” (Figure 3A), all lost the F404L mutation in long term growth (Supplementary Figure 5), likely suggesting a subclonal mutation that was outcompeted by the F404F wildtype clone in long-term growth in the absence of fulvestrant.

Compound F404 mutations are sensitive to novel SERDs.

In silico analysis of binding energies suggested mutations at F404L may increase the binding affinity of second-generation oral SERDs (Supplementary Table 1). Therefore, we investigated if fulvestrant resistance generated through compound F404 mutations could be overcome by novel SERDs in clinical development, or by the selective estrogen receptor modulator (SERM) tamoxifen. All novel SERDS investigated were active against CRISPR models with both single F404L mutations and D538G+F404L compound mutations, including elacestrant, camizestrant, 4OH tamoxifen and giredestrant (Figure 6A-E, Table 1; Supplementary Figures 6-9). In particular, models with D538G+F404L compound mutations that were overtly resistant to fulvestrant, showed sensitivity to other SERD/SERMs comparable to other D538G expressing models (Figure 6A-E; Supplementary Figures 6-9). Similarly, elacestrant, camizestrant, 4OH tamoxifen or giredestrant all fully inhibited ERE activity following transient transfection of D538G+F404L and E380Q+F404L (Figure 6F), despite transfection of these compound mutations resulting in substantial resistance to fulvestrant. Interestingly, 4OH tamoxifen did not completely suppress activity of the ERE reporter gene assay, with ~10-20% activity irrespective of *ESR1* mutation (Figure 6F), potentially reflecting the difference in mechanism of action between it and the SERDs.

Discussion

Here, we present a robust genomic analysis of resistance to fulvestrant in *ESR1* mutant breast cancer using paired circulating tumour DNA sequencing in patients treated with fulvestrant in the plasmaMATCH study(17). We identify novel *ESR1* mutations that alter F404, that occur only in patients treated with fulvestrant with pre-existing activating *ESR1* mutations in their cancer. F404 mutations are acquired in *cis* with a pre-existing activating *ESR1* mutation, with the resulting compound mutation resulting in profound resistance to fulvestrant, but with retained sensitivity to a range of novel SERDs, identifying a treatment strategy to overcome acquired resistance conveyed by F404 mutations.

Mutations at F404 do not appear to occur in the absence of fulvestrant exposure, and then also only in the presence of other activating *ESR1* mutations. F404 has previously been predicted to form *pi*-stacking bonds with plant polyphenols identified in a screen of compounds as candidates with anti-estrogenic properties (24). Similarly, structural analysis suggested that F404 forms a *pi*-stacking bond with an aromatic ring in both estradiol and fulvestrant. Consistent with these predictions, *in vitro,* the introduction of F404 mutations resulted in lower levels of ERE activity compared to wildtype *ESR1* (Figure 3). Mutation of F404 would likely reduce *ESR1* activity in the absence of other *ESR1* mutations, which may have a deleterious effect on tumour growth, explaining the lack of F404 mutations observed without prior acquisition of an activating *ESR1* mutation. Compound F404 mutations resulted in profound resistance to fulvestrant, with single F404 mutant models showing more limited fulvestrant resistance. It is likely that the effect of *ESR1* activating mutations on the ligand binding pocket, combined with the loss of the *pi*-stacking bond, result in

an impairment of fulvestrant affinity for the ligand binding pocket. *In silico* analysis of binding energies was consistent with this hypothesis, although formal *in vitro* studies in the future would be required to assess this (Supplementary Table 1), with the alternative hypothesis being that F404X mutations do not impact the binding of fulvestrant, but impact the conformational change induced by fulvestrant binding. Interesting *in silico* analysis predicted that binding energies of novel SERDs were not affected by, or even promoted by, F404 mutations, and consistent with this the efficacy of novel SERDs, was unaffected by mutations in F404, providing a therapeutic option to circumvent this mechanism of resistance. Investigation of a wider range of SERDs/SERMs is required to confirm whether this resistance mutation is, as is currently suggested, specific to fulvestrant. This endocrine therapy resistance mechanism is unique in leading to re-activation of the estrogen receptor itself, in contrast to other mechanisms such as inactivating *NF1* and *ARID1A* mutations (25,26), emphasising the need to identify whether further drug specific mutations may limit the efficacy of oral ER degraders in clinical development.

Interestingly, our results predict that although F404 compound mutations promote growth in the presence of fulvestrant, this conditional advantage may come at the come at the cost of reduced fitness in the absence of fulvestrant, as F404 mutations may reduce ER signalling in the absence of fulvestrant and therefore come at the cost of impaired clonal growth once fulvestrant is withdrawn (Supplementary Figure 5). This suggests that for patients with resistance to fulvestrant generated by F404 mutations, there may be the possibility of rechallenging with fulvestrant after a treatment break, as has been seen rechallenging with cetuximab in patients who *KRAS* mutations in colorectal cancer(27).

Our study emphasises the extent to which tumour genomes may evolve through fulvestrant therapy, with 25% patients acquiring a potentially targetable driver mutation. Evidence suggests that ER positive breast cancers may become substantially heterogeneous after progression on endocrine therapy, and that heterogeneity presents a considerable challenge to subsequent treatment efficacy (21,28,29). The high incidence of mutation 'acquisition' was largely driven by gain of *ESR1* mutations, and likely reflects clonal selection in the cancer, whilst emphasising the importance of ctDNA liquid biopsy testing to match treatment to current genomics (17). This heterogeneity may be more marked in *ESR1* mutant cancer, as *ESR1* mutations may co-occur with other mechanisms of genetic resistance, potentially reflecting cancers that are pre-disposed to acquiring genetic mechanisms of resistance (21,29) Recently, acquisition of secondary mutations in *cis* with hotspot driver mutations in *PIK3CA* were described (30), leading to increased signalling and tumour growth. *PIK3CA* double mutants were found to have increased sensitivity to PI3K inhibitors (30). Similarly, we report double mutations in *ESR1* where the primary mutation has been widely described (11,19,21,29,31), acquired in response to exposure to aromatase inhibitors (7). In contrast to *PIK3CA* double mutations which enhance PI3K signalling, acquisition of F404 only provides a growth advantage in the context of exposure to fulvestrant.

In conclusion, we identify a novel *ESR1* mutation at ERα F404, that when acquired in combination with an activating *ESR1* mutation induces resistance to the widely used SERD fulvestrant. Mutations at this codon result in changes at F404 to amino acid residues which lack an aromatic ring, disrupting the *pi*-stacking bond with both estradiol and fulvestrant. The resistance of F404 double mutants is specific to fulvestrant and can be overcome by use of alternate SERDs, suggesting a route to

overcome therapeutic resistance in the clinic. Mutations in the estrogen receptor can confer resistance to ER binding drugs, without promoting ER activity, identifying a new mechanism through which the cancer can become resistant to hormonal therapies.

Materials and Methods

Patient enrolment into plasmaMATCH and blood sampling

The plasmaMATCH trial (NCT03182634). was co-sponsored by the Institute of Cancer Research and the Royal Marsden National Health Service (NHS) Foundation Trust, London, UK, and approved by a Research Ethics Committee (16/SC/0271), as previously reported (17). Baseline ctDNA testing was conducted with droplet digital PCR (ddPCR), and from partway through the trial with targeted sequencing in parallel to ddPCR. For patients enrolled prior to prospective targeted sequencing, a banked pre-treatment plasma sample was retrospectively sequenced. An additional plasma sample taken at disease progression was also subject to targeted sequencing.

For the baseline ctDNA test, 30-40ml of blood was collected in 3–4 10ml cell-free DNA BCT Streck tubes. 30ml of blood was shipped at ambient temperature to a central laboratory (Centre for Molecular Pathology, Royal Marsden Hospital) for ddPCR testing and retrospective targeted sequencing. In addition, from partway through the trial 10ml blood were shipped to Guardant Health (Redwood City, California, USA) for targeted sequencing. An additional sample was collected at cycle 1 day1, and end of treatment sample in 2 x 10mL BD Vacutainer® EDTA tubes, centrifuged within 1 hour of collection, for retrospective targeted sequencing.

Computer modeling of estrogen *pi*-stacking with ER

Models of estrogen ligand A-ring *pi*-stacking with F404 in the ligand binding pocket of ERα were generated as follows: There is no crystal structure for fulvestrant bound to ERα; the only related crystal structure is for ICI 164,384, a close fulvestrant analog, in the other ER subtype, ERβ (PDB ID 1HJ1). Therefore, we removed the ICI

164,384 ligand from this structure, modified the side chain to match that of fulvestrant, and modelled it into the ERα crystal structure for the antiestrogen Bazedoxifene after removing the Bazedoxifene ligand (PDB ID 6PSJ); the fitting was done using Schrödinger Glide (https://www.schrodinger.com/products/glide). The estradiol structure in ERα is from PDB ID 3UUD.

ctDNA testing and analysis.

ctDNA targeted sequencing was conducted with Guardant360 that identifies single nucleotide variants (SNVs), indels, copy number alterations and fusions within protein-coding regions of 73 (version 2.10) or 74 genes (version 2.11), as previously described(29,32).

Variants from Guardant 360 were annotated with VEP version 96(33). Germline calls were identified by Guardant360 with additional calls (identified based on a combination of VAF frequency around 50%+− 2% and VAF in general population in the Genome Aggregation Database >0.001%) excluded. To identify pathogenic mutations, variants were annotated with OncoKB(34) and CancerHotspots(35). Mutations were classified as pathogenic based on Cancer Hotspots or OncoKB annotations or recurrent mutations in key breast cancer genes (*ESR1*, *HER2*, *PIK3CA*, *EGFR*, *RB1* and *FGFR2*) or splicing mutations. All analyses presented are based on mutations assessed as likely pathogenic. Targetability was assigned using OncoKB annotation, a manually curated database of alterations(34).

Cell Lines

MCF7 cell lines were obtained from ATCC and cultured in phenol free RPMI media (32404-014, Life technologies) supplemented with 10% dextran/charcoal stripped FBS (12676029, Life Technologies), 1nM oestradiol (Sigma), glutamine (25030149,

Life technologies), penicillin and streptomycin (15140-122, Life technologies). Cell lines were banked in multiple aliquots on receipt to reduce risk of phenotypic drift and identity confirmed by STR profiling with the PowerPlex 1.2 System (Promega). Cell cultures were routinely tested for presence of mycoplasma using MycoAlert® Detection kit (LT07-318 Lonza).

Antibodies and Drugs

Antibodies used were ERα (sc543, Santa Cruz Biotechnology), PGR (8757, Cell Signaling Technology), TFF1 (15571, Cell Signaling Technology) and βactin (A5441 Sigma). Secondary antibodies used were α-rabbit-HRP (7074) and α-mouse-HRP (7076, Cell Signaling Technology). Fulvestrant (S1191), 4OH-tamoxifen (S7827) and camizestrant (S8958) were obtained from Selleck Chemicals. Elacestrant (HY-19822A) and giredestrant (HY-109176) were obtained from MedChemExpress.

Generation and analysis of *ESR1* mutant CRISPR models

MCF7 cells were subjected to CRISPR-Cas9 genome editing with homology-directed repair (HDR) using Integrated DNA Technologies' (IDT) Alt-R™ CRISPR-Cas9 system according to manufacturer's guidelines. Briefly, the day before transfection 250,000 cells were plated per well of a 6 well plate in antibiotic free media containing HDR enhancer V2 (2μM, 10007910 IDT). crRNA and HDR templates were designed using IDT's Alt-R™ CRISPR HRD design tool (https://eu.idtdna.com/pages/tools/alt-r-crispr-hdr-design-tool; Supplementary table 2). gRNA complexes (1μM) were prepared by hybridisation of targeting crRNA with tracrRNA-ATTO555 (1075928, IDT). Ribonucleoprotein (RNP) complexes were prepared by addition of gRNA complexes, Cas9 (1081060 IDT), HDR template, Cas9 PLUS reagent (ThermoFisher Scientific), and OptiMEM (31985062, ThermoFisher Scientific), and incubated for 5min at room temperature. Transfection mixes were prepared using RNP complexes with

Lipofectamine™ CRISPMAX™ (CMAX00008, ThermoFisher Scientific) and incubated for 20mins at room temperature. Transfection mixes were added to pre-seeded cells in 6 well plates and incubated overnight. 48h post transfection cells were spilt into 10cm dishes and cells cultured until colonies had established. gDNA was extracted from the transfection pool using QuickExtract™ DNA Extraction Solution (QE09050 Lucigen) and CRISPR editing assessed using Alt-R Genome Editing Detection kit (1075932 IDT). After approximately 2 weeks individual colonies were picked into 96 well plates and expanded. gDNA was extracted from colonies using QuickExtract™ DNA Extraction Solution (QE09050 Lucigen), subjected to PCR (primer details in Supplementary table 1), PCR products isolated (QIAquick PCR purification kit, 28104 Qiagen) and screened for presence of targeted mutations by Sanger sequencing (Azenta Life Sciences). Clones in which targeted mutations were identified were expanded.

To confirm mutant *ESR1* variants were expressed by selected clones, RNA was extracted using RNeasy Mini Kit (74104, Qiagen), cDNA prepared using SuperScript IV first strand synthesis kit (18091050, ThermoFisher Scientific) and amplified using AllTaq PCR Core Kit (203123, Qiagen; primer details in Supplementary table 1). As described, PCR products were isolated and screened for presence of targeted mutations by Sanger sequencing (Azenta Life Sciences).

Fulvestrant Screen of *ESR1* mutant expressing MCF7 cells

A series of expression constructs with *ESR1* point mutations was generated in the pcDNA3.1 HA-ERα (18). Transfections of MCF7 cells using HA-tagged wild-type or mutant ERα, with 3×-ERE-TATA-Luciferase reporter and pRL-TK-Renilla luciferase plasmid (Promega) using Lipofectamine 2000 (Life technologies) were done according to the methods of Toy et al 2013 (18). Cells were exposed to fulvestrant at

indicated concentrations 1 day after transfection for 24h, and luciferase activities were determined using the Dual® Luciferase Reporter Assay System (E2920, Promega) according to the manufacturer's instructions. Luciferase bioluminescence measurements were performed with the Veritas Microplate Luminometer (Promega).

ERE assays with transient transfection

pcDNA3.1+/C-DYK plasmids, with the open reading frame of *ESR1* (NM_000125.4) with and without point mutations (estrogen receptor constructs, ERCs; Supplementary Table 2), were purchased from GenScript (The Netherlands). Sanger sequencing was used to confirm the presence of the desired mutations within the custom insert. MCF-7 cells were seeded in 6 well plates with 250,000 cells per well in antibiotic free media, the following day transfected using Fugene 6 (Promega, USA) with the ERC, a plasmid expressing an estrogen response element with firefly luciferase (ERE-luciferase) (36) and pRL-CMV (*Renilla* luciferase control, Promega). 24 hours post transfection, experimental conditions were applied for a further 24h, and firefly luciferase (ERE activity) and *Renilla* luciferase using the Dual-Glo® Luciferase Assay System (E2920, Promega) following the manufacturer's instructions measured with a VICTOR X3 MultiLab. Experiments were repeated a minimum of 3 times.

In Vitro Viability Assessment

Colony formation assays were conducted in 6-well plates, seeded with 10,000 cells/well prior to exposure to the indicated experimental conditions. Plates were fixed with tricyclic acid (10%$^{v}/_{v}$), stained with sulforhodamine B (S1402, Sigma; 0.37% $^{w}/_{v}$, in 1% acetic acid) and colonies counted using a GelCOUNT instrument (Oxford Technologies). For short-term survival assays, 700cells/well were plated in

384 well plates and exposed to indicated drugs. Survival was assessed after 6 days of treatment using CellTiter-Glo cell viability assay (G7572, Promega).

Western Blotting

Cells were lysed in NP40 lysis buffer (1% v/v NP40, 10 mmol/L Tris–Cl pH8, 150 mmol/L NaCl, 1 mmol/L EDTA, 1 mmol/L DTT) supplemented with protease/phosphatase inhibitor cocktail (5872, Cell Signaling Technologies). Western blots were carried out with precast Bis-Tris gels (Life Technologies).

RNAseq expression analysis

ESR1 mutant models and controls were treated with 1nM estradiol ± 1μM fulvestrant for 24hr (9 models with estradiol treatment, 7 of which also had fulvestrant treatment, n=3), cells harvested, and RNA extracted using RNeasy Mini Kit (74104, Qiagen). Each cell model was treated in 3 independent experiments.

48 total RNA samples were sent to Novogene (UK) Company Ltd and subjected to Eukaryotic mRNA-Seq (Illumina Novaseq PE150, Q30 ≥ 80%). Sequencing data for 48 RNA samples for 9 models using bcbio-nextgen,1.2.4 pipeline, reads were aligned using STAR with version STAR 2.6.1d, counted using salmon,1.4.0. The data was divided in two parts with respect to treatment with 1nM estradiol and 1μM fulvestrant as EST and FUL. The data normalized using DEseq2 version '1.38.3'. DESeq2 was also used to determine differentially expressed genes between different model of single mutants (404_D10, 538_D6C) versus control (MCF7), single mutants (404_D10, 538_D6C) versus wt_D11 and double mutants (538_404, 404_538) vs single mutants (538_D6C, 404_D10) using shrunken log2 fold changes in EST and FUL data respectively. Heatmaps were generated using pheatmap package version '1.0.12'and ggplots '3.4.2' R package. GSEA analysis was carried

out using Molecular Signatures Database 'Hallmarks' gene set collection using package fgsea '1.24.0' and clusterProfiler '4.6.2' R packages.

Statistical analyses

Statistical analysis was carried out using R version 4.0.5 and GraphPad Prism v8.4.3. Time to event survival data were analysed with log-rank test and hazard ratios were calculated with Cox regression. Plots were created using GraphPad Prism v8.4.3 and the R software packages ggplot2 and survminer.

Data Availability Statement

The processed plasmaMATCH Guardant360 sequencing data generated and analysed during the current study are available as part of Kingston B, *et al* 2021 (29). We do not have permission from the patients to publicly deposit the raw sequencing data. To protect the privacy and confidentiality of patients in this study, clinical data are also not made publicly available. The data can be obtained by submitting a formal data access request in accordance with the Institute of Cancer Research Clinical Trials and Statistics Unit (ICR-CTSU) data and sample access policy. Requests are to be made via a standard proforma describing the nature of the proposed research and extent of data requirements which is reviewed by the trial management group. Data recipients are required to enter a formal data sharing agreement, which describes the conditions for data release and requirements for data transfer, storage, archiving, publication, and intellectual property. Trial documentation including the protocol are available on request by contacting plasmamatch-icrctsu@icr.ac.uk.

Acknowledgments

This research was funded by Cancer Research UK and Breast Cancer Now, and sequencing of ctDNA was conducted by Guardant Health. The plasmaMATCH trial is funded by Cancer Research UK (CRUK/15/010, C30746/A19505), with additional support from AstraZeneca, Puma Biotechnology, Guardant Health and BioRad. Grateful thanks to all trial participants and their families. We thank Breast Cancer Now for funding this work as part of Programme Funding to the Breast Cancer Now Toby Robins Research Centre. This study represents independent research supported by the NIHR Biomedical Research Centre at The Royal Marsden NHS Foundation Trust and the Institute of Cancer Research, London.

This study was presented in part at the 2022 American Society of Clinical Oncology 3-7th June 2022, J Clin Oncol 40, 2022 (suppl 16; abstr 1009), https://doi.org/10.1200/JCO.2022.40.16_suppl.1009.

References

1. Turner NC, Ro J, Andre F, Loi S, Verma S, Iwata H*, et al.* Palbociclib in Hormone-Receptor-Positive Advanced Breast Cancer. N Engl J Med **2015**;373(3):209-19 doi 10.1056/NEJMoa1505270.
2. Andre F, Ciruelos E, Rubovszky G, Campone M, Loibl S, Rugo HS*, et al.* Alpelisib for PIK3CA-Mutated, Hormone Receptor-Positive Advanced Breast Cancer. N Engl J Med **2019**;380(20):1929-40 doi 10.1056/NEJMoa1813904.

3. Sledge GW, Jr., Toi M, Neven P, Sohn J, Inoue K, Pivot X*, et al.* The Effect of Abemaciclib Plus Fulvestrant on Overall Survival in Hormone Receptor-Positive, ERBB2-Negative Breast Cancer That Progressed on Endocrine Therapy-MONARCH 2: A Randomized Clinical Trial. JAMA Oncol **2020**;6(1):116-24 doi 10.1001/jamaoncol.2019.4782.
4. Osborne CK, Wakeling A, Nicholson RI. Fulvestrant: an oestrogen receptor antagonist with a novel mechanism of action. Br J Cancer **2004**;90 Suppl 1:S2-6 doi 10.1038/sj.bjc.6601629.
5. Katzenellenbogen JA, Mayne CG, Katzenellenbogen BS, Greene GL, Chandarlapaty S. Structural underpinnings of oestrogen receptor mutations in endocrine therapy resistance. Nat Rev Cancer **2018**;18(6):377-88 doi 10.1038/s41568-018-0001-z.
6. Guan J, Zhou W, Hafner M, Blake RA, Chalouni C, Chen IP*, et al.* Therapeutic Ligands Antagonize Estrogen Receptor Function by Impairing Its Mobility. Cell **2019**;178(4):949-63 e18 doi 10.1016/j.cell.2019.06.026.
7. Schiavon G, Hrebien S, Garcia-Murillas I, Cutts RJ, Pearson A, Tarazona N*, et al.* Analysis of ESR1 mutation in circulating tumor DNA demonstrates evolution during therapy for metastatic breast cancer. Sci Transl Med **2015**;7(313):313ra182 doi 10.1126/scitranslmed.aac7551.
8. Spoerke JM, Gendreau S, Walter K, Qiu J, Wilson TR, Savage H*, et al.* Heterogeneity and clinical significance of ESR1 mutations in ER-positive metastatic breast cancer patients receiving fulvestrant. Nat Commun **2016**;7:11579 doi 10.1038/ncomms11579.
9. Turner NC, Swift C, Kilburn L, Fribbens C, Beaney M, Garcia-Murillas I*, et al.* ESR1 Mutations and Overall Survival on Fulvestrant versus Exemestane in Advanced Hormone Receptor-Positive Breast Cancer: A Combined Analysis of the Phase III SoFEA and EFECT Trials. Clin Cancer Res **2020**;26(19):5172-7 doi 10.1158/1078-0432.CCR-20-0224.
10. Turner NC, Swift C, Kilburn L, Fribbens C, Beaney M, Garcia-Murillas I*, et al.* ESR1 Mutations and Overall Survival on Fulvestrant versus Exemestane in Advanced Hormone Receptor–Positive Breast Cancer: A Combined Analysis of the Phase III SoFEA and EFECT Trials. Clinical Cancer Research **2020**;26(19):5172-7 doi 10.1158/1078-0432.Ccr-20-0224.
11. Toy W, Weir H, Razavi P, Lawson M, Goeppert AU, Mazzola AM*, et al.* Activating ESR1 Mutations Differentially Affect the Efficacy of ER Antagonists. Cancer Discov **2017**;7(3):277-87 doi 10.1158/2159-8290.CD-15-1523.
12. Bihani T, Patel HK, Arlt H, Tao N, Jiang H, Brown JL*, et al.* Elacestrant (RAD1901), a Selective Estrogen Receptor Degrader (SERD), Has Antitumor Activity in Multiple ER(+) Breast Cancer Patient-derived Xenograft Models. Clin Cancer Res **2017**;23(16):4793-804 doi 10.1158/1078-0432.CCR-16-2561.
13. Liang J, Zbieg JR, Blake RA, Chang JH, Daly S, DiPasquale AG*, et al.* GDC-9545 (Giredestrant): A Potent and Orally Bioavailable Selective Estrogen Receptor Antagonist and Degrader with an Exceptional Preclinical Profile for ER+ Breast Cancer. J Med Chem **2021**;64(16):11841-56 doi 10.1021/acs.jmedchem.1c00847.
14. Scott JS, Moss TA, Balazs A, Barlaam B, Breed J, Carbajo RJ*, et al.* Discovery of AZD9833, a Potent and Orally Bioavailable Selective Estrogen Receptor Degrader and Antagonist. J Med Chem **2020**;63(23):14530-59 doi 10.1021/acs.jmedchem.0c01163.

15. Di Leo A, Jerusalem G, Petruzelka L, Torres R, Bondarenko IN, Khasanov R*, et al.* Final overall survival: fulvestrant 500 mg vs 250 mg in the randomized CONFIRM trial. J Natl Cancer Inst **2014**;106(1):djt337 doi 10.1093/jnci/djt337.
16. Patani N, Dunbier AK, Anderson H, Ghazoui Z, Ribas R, Anderson E*, et al.* Differences in the transcriptional response to fulvestrant and estrogen deprivation in ER-positive breast cancer. Clin Cancer Res **2014**;20(15):3962-73 doi 10.1158/1078-0432.CCR-13-1378.
17. Turner NC, Kingston B, Kilburn LS, Kernaghan S, Wardley AM, Macpherson IR*, et al.* Circulating tumour DNA analysis to direct therapy in advanced breast cancer (plasmaMATCH): a multicentre, multicohort, phase 2a, platform trial. Lancet Oncol **2020**;21(10):1296-308 doi 10.1016/S1470-2045(20)30444-7.
18. Toy W, Shen Y, Won H, Green B, Sakr RA, Will M*, et al.* ESR1 ligand-binding domain mutations in hormone-resistant breast cancer. Nat Genet **2013**;45(12):1439-45 doi 10.1038/ng.2822.
19. Robinson DR, Wu YM, Vats P, Su F, Lonigro RJ, Cao X*, et al.* Activating ESR1 mutations in hormone-resistant metastatic breast cancer. Nat Genet **2013**;45(12):1446-51 doi 10.1038/ng.2823.
20. Harrod A, Lai CF, Goldsbrough I, Simmons GM, Oppermans N, Santos DB*, et al.* Genome engineering for estrogen receptor mutations reveals differential responses to anti-estrogens and new prognostic gene signatures for breast cancer. Oncogene **2022**;41(44):4905-15 doi 10.1038/s41388-022-02483-8.
21. O'Leary B, Cutts RJ, Liu Y, Hrebien S, Huang X, Fenwick K*, et al.* The Genetic Landscape and Clonal Evolution of Breast Cancer Resistance to Palbociclib plus Fulvestrant in the PALOMA-3 Trial. Cancer Discov **2018**;8(11):1390-403 doi 10.1158/2159-8290.CD-18-0264.
22. Pascual J, Lim JSJ, Macpherson IR, Armstrong AC, Ring A, Okines AFC*, et al.* Triplet Therapy with Palbociclib, Taselisib, and Fulvestrant in PIK3CA-Mutant Breast Cancer and Doublet Palbociclib and Taselisib in Pathway-Mutant Solid Cancers. Cancer Discov **2021**;11(1):92-107 doi 10.1158/2159-8290.CD-20-0553.
23. Mafalda Oliveira EPH, Jason Incorvati, Begoña Bermejo de la Heras, Emiliano Calvo, Javier García-Corbacho, Manuel Ruiz-Borrego, Christos Vaklavas, Nicholas C. Turner, Eva M. Ciruelos, Manish R. Patel, Anne C. Armstrong, Peter Kabos, Chris Twelves, Tim Brier, Itziar Irurzun-Arana, Teresa Klinowska, Justin P.O. Lindemann, Christopher J. Morrow, Richard D. Baird. Serena-1: Updated analyses from a phase 1 study (parts C/D) of the next-generation oral SERD camizestrant (AZD9833) in combination with palbociclib, in women with ER-positive, HER2-negative advanced breast cancer. Journal of Clinical Oncology **2022**;40(16_suppl):1032 doi 10.1200/JCO.2022.40.16_suppl.1032.
24. Yugandhar P, Kumar KK, Neeraja P, Savithramma N. Isolation, characterization and in silico docking studies of synergistic estrogen receptor a anticancer polyphenols from Syzygium alternifolium (Wt.) Walp. J Intercult Ethnopharmacol **2017**;6(3):296-310 doi 10.5455/jice.20170709031835.
25. Nagarajan S, Rao SV, Sutton J, Cheeseman D, Dunn S, Papachristou EK*, et al.* ARID1A influences HDAC1/BRD4 activity, intrinsic proliferative capacity and breast cancer treatment response. Nat Genet **2020**;52(2):187-97 doi 10.1038/s41588-019-0541-5.
26. Pearson A, Proszek P, Pascual J, Fribbens C, Shamsher MK, Kingston B*, et al.* Inactivating NF1 Mutations Are Enriched in Advanced Breast Cancer and

Contribute to Endocrine Therapy Resistance. Clin Cancer Res **2020**;26(3):608-22 doi 10.1158/1078-0432.CCR-18-4044.
27. Siravegna G, Mussolin B, Buscarino M, Corti G, Cassingena A, Crisafulli G*, et al.* Clonal evolution and resistance to EGFR blockade in the blood of colorectal cancer patients. Nat Med **2015**;21(7):795-801 doi 10.1038/nm.3870.
28. Razavi P, Chang MT, Xu G, Bandlamudi C, Ross DS, Vasan N*, et al.* The Genomic Landscape of Endocrine-Resistant Advanced Breast Cancers. Cancer Cell **2018**;34(3):427-38 e6 doi 10.1016/j.ccell.2018.08.008.
29. Kingston B, Cutts RJ, Bye H, Beaney M, Walsh-Crestani G, Hrebien S*, et al.* Genomic profile of advanced breast cancer in circulating tumour DNA. Nat Commun **2021**;12(1):2423 doi 10.1038/s41467-021-22605-2.
30. Vasan N, Razavi P, Johnson JL, Shao H, Shah H, Antoine A*, et al.* Double PIK3CA mutations in cis increase oncogenicity and sensitivity to PI3Kalpha inhibitors. Science **2019**;366(6466):714-23 doi 10.1126/science.aaw9032.
31. Fribbens C, O'Leary B, Kilburn L, Hrebien S, Garcia-Murillas I, Beaney M*, et al.* Plasma ESR1 Mutations and the Treatment of Estrogen Receptor-Positive Advanced Breast Cancer. J Clin Oncol **2016**;34(25):2961-8 doi 10.1200/JCO.2016.67.3061.
32. Odegaard JI, Vincent JJ, Mortimer S, Vowles JV, Ulrich BC, Banks KC*, et al.* Validation of a Plasma-Based Comprehensive Cancer Genotyping Assay Utilizing Orthogonal Tissue- and Plasma-Based Methodologies. Clin Cancer Res **2018**;24(15):3539-49 doi 10.1158/1078-0432.CCR-17-3831.
33. McLaren W, Gil L, Hunt SE, Riat HS, Ritchie GR, Thormann A*, et al.* The Ensembl Variant Effect Predictor. Genome Biol **2016**;17(1):122 doi 10.1186/s13059-016-0974-4.
34. Chakravarty D, Gao J, Phillips SM, Kundra R, Zhang H, Wang J*, et al.* OncoKB: A Precision Oncology Knowledge Base. JCO Precis Oncol **2017**;1:1-16 doi 10.1200/PO.17.00011.
35. Chang MT, Asthana S, Gao SP, Lee BH, Chapman JS, Kandoth C*, et al.* Identifying recurrent mutations in cancer reveals widespread lineage diversity and mutational specificity. Nat Biotechnol **2016**;34(2):155-63 doi 10.1038/nbt.3391.
36. Martin LA, Farmer I, Johnston SR, Ali S, Marshall C, Dowsett M. Enhanced estrogen receptor (ER) alpha, ERBB2, and MAPK signal transduction pathways operate during the adaptation of MCF-7 cells to long term estrogen deprivation. J Biol Chem **2003**;278(33):30458-68 doi 10.1074/jbc.M305226200.
37. Zhou X, Edmonson MN, Wilkinson MR, Patel A, Wu G, Liu Y*, et al.* Exploring genomic alteration in pediatric cancer using ProteinPaint. Nat Genet **2016**;48(1):4-6 doi 10.1038/ng.3466.

Table 1. Calculated IC50 and EC50 of 4OH tamoxifen and novel SERDs in *ESR1* mutant models.

		MCF7	WT D11	F404L D10	D538G D6C	404 538 1EF	538 404 30EF	538 404 34EF	538 404 36EF	538 404 37EF
Elacestrant	IC50 (nM)	12.2	3.9	5.4	27.7	20.1	23.3	34.6	nc	35.5
	EC50 (nM)	16.2	10.7	6.9	59.0	24.9	27.5	46.3	67.0	57.8
Camizestrant	IC50 (nM)	1.0	0.7	1.8	14.0	9.6	9.9	15.1	7.5	15.8
	EC50 (nM)	2.5	2.2	2.2	28.8	10.9	12.2	20.8	47.2	25.3
4OH tamoxifen	IC50 (nM)	5.6	1.2	1.4	16.8	10.3	8.7	14.4	11.1	20.6
	EC50 (nM)	8.9	7.1	3.4	37.9	14.9	11.8	21.7	95.3	46.9
Giredestrant	IC50 (nM)	1.2	0.3	0.4	3.1	2.5	2.5	3.7	1.0	4.2
	EC50 (nM)	1.3	0.8	0.5	6.3	3.1	3.2	4.6	9.2	6.9

nc not calculated

Figures

Figure 1. Baseline *ESR1* mutations and fulvestrant efficacy

A. % Incidence of mutations in indicated genes at baseline in Cohort A (n=79 assessable patients).

B. Incidence of baseline *ESR1* alterations within Cohort A (n=79 assessable patients).

C. Progression-free survival of patients in Cohort A, divided by baseline *ESR1* Y537C mutation status (left) and *ESR1* Y537S mutation status (right). p-values from log rank test. HR >1 denotes worse PFS for that group. WT, wild type; mt, mutant

D. MCF7 cells were co-transfected with the indicated *ESR1* expression constructs and treated with the indicated concentration of fulvestrant in the presence of 1nM estradiol for 24 hours and ERE-luciferase reporter activity determined. 2 independent experiments.

Figure 2. Acquired mutations on Fulvestrant.

A. incidence of acquired alterations (n=69 assessable patients), coloured by targetability of the alterations (methods). Level 2B denotes the highest level of supporting evidence ("Standard care biomarker recommended by the NCCN or other professional advice guidelines predictive of response to an FDA-approved drug"), while Level 4 is the lowest ("Compelling biochemical evidence supports the biomarker as being predictive of response to a drug").

B. incidence of acquired *ESR1* mutations (n=14 patients), and resultant amino acid changes.

C. *ESR1* F404 locus in the DNA-binding domain of the estrogen receptor. The number of base changes identified within the dataset that result in the three different missense mutations are illustrated using https://proteinpaint.stjude.org/ (37).

D. *cis/trans* analysis of F404 and E380Q in the three patients with assessable targeted sequencing data. Both alleles of chromosome 6 are represented, with annotated location of the F404 and E380Q on each respective allele representing the *cis/trans* relationship of the variants.

E, Mutations at phenylalanine 404 result in substitution of amino acid residues without an aromatic ring.

F, *In silico* modelling predicts the aromatic ring of F404 contributes to a *pi*-stacking bond between the receptor and both estrogen and fulvestrant.

Figure 3. F404 does not activate estrogen signalling.

A. CRISPR clones of MCF7 cells expressing *ESR1* F404L (1210T>C, CRISPR edit indicated by red arrows) or D538G (1613A>G; CRISPR edit indicated by black arrows) were identified by RT-PCR followed by Sanger sequencing (left hand panels). Similarly, a second round of CRISPR was used to introduce *ESR1* F404L (1210T>C) into a clone (D6C) that expressed D538G (1613A>G; right hand panels).

B. Estrogen dependent growth was assessed in colony formation assay. Parental MCF7 cells and indicated *ESR1* mutant models were grown in either the absence or presence of estradiol (1nM) for 14 days.

C. Quantification of colony formation assays of *ESR1* mutant models treated with and without estradiol (1nM). SRB stained colonies were dissolved and absorbance at

565nm measured. Mean with sem, n=3 independent experiments, nonparametric one way ANOVA with Dunn's multiple comparisons test, **P<0.01.

D. Expression of estrogen target genes, progesterone receptor (PgR) and trefoil factor-1 (TFF1), assessed by western blot in parental MCF7 cells and indicated *ESR1* mutant models grown in either the absence or presence of estradiol (1nM) for 24 hours.

E. MCF7 cells were transfected with *ESR1* expression constructs with indicated *ESR1* variants. Expression of ERα was determined by western blot.

F. MCF7 cells were co-transfected with the indicated *ESR1* expression constructs ERE-luciferase reporter and control construct. Cells were treated in either the absence or presence of estradiol (1nM) for 24 hours and ERE-luciferase activity assessed. 2-way repeated measures ANOVA with Dunnett's multiple comparisons test, n=4 mean with SD, *P<0.05.

Figure 4. Compound F404L mutations induces resistance to fulvestrant.

A. Compound mutations of D538G-F404L in MCF7 cells, along with single mutations and wildtype, with sensitivity to fulvestrant assessed after 6 days treatment with Cell Titre Glo viability assay. N=4 mean with SD.

B. Representative images of clonongenic assays grown in indicated concentrations of fulvestrant for 14 days.

C. Quantification of colony formation assays for *ESR1* mutant models treated with the indicated concentrations of fulvestrant for 14 days. EC50 and IC50 values were

calculated from the response curves. SRB stained colonies were dissolved and absorbance at 565nm measured. Mean with sem, n=3 independent experiments.

D. Expression of estrogen target genes, progesterone receptor (PgR) and trefoil factor-1 (TFF1), assessed by western blot in parental MCF7 cells and indicated *ESR1* mutant models grown in the presence of 1nM estradiol or 1μM fulvestrant.

E. MCF7 cells were co-transfected with the indicated *ESR1* expression constructs ERE-luciferase reporter and control construct. Cells were treated with 1nM estradiol either the absence or presence of fulvestrant (1μM) for 24 hours and ERE-luciferase activity assessed. 2-way repeated measures ANOVA with Sidak's multiple comparisons test, n=4 mean with SD, **P<0.01, ***P<0.001, ****P<0.0001.

Figure 5. Transcriptomic analysis of *ESR1* mutant models

A, Gene set enrichment analysis for D538G+F404L models compared to D538G D6C cells maintained in 1nM estradiol. Pathways highlighted red, false discovery rate adjusted q value <0.05.

B, Gene set enrichment analysis for D538G+F404L models compared to D538G D6C cells treated with 1μM fulvestrant for 24hr. Pathways highlighted red, false discovery rate adjusted q value <0.05.

C, Gene Set Enrichment Analysis (GSEA) for *ESR1* mutant models. Normalised enrichment score (NES) is shown for the indicated pathways. *False discovery rate adjusted q value <0.05.

D, Heat map of "Estrogen response late" genes (Log2 expression) for *ESR1* mutant models maintained in 1nM estradiol.

E, Heat map of “Estrogen response late” genes (Log2 expression) for *ESR1* mutant models treated with 1μM fulvestrant in presence of 1nMestradiol.

Figure 6. Compound F404 mutations are sensitive to novel SERDs.

A-D. Compound mutations of D538G-F404L in MCF7 cells, along with single mutations and wildtype, with sensitivity to elacestrant (A), camizestrant (B), 4OH tamoxifen (C) and giredestrant (D), assessed after 6 days treatment with Cell Titre Glo viability assay. N=4 mean with SD.

E. Representative clonongenic assays grown in indicated concentrations of elacestrant, camizestrant, 4OH tamoxifen and giredestrant for 14 days.

F. MCF7 cells were co-transfected with the indicated *ESR1* expression constructs ERE-luciferase reporter and control construct. Cells were treated with indicated concentrations of fulvestrant, elacestrant, camizestrant, 4OH tamoxifen and giredestrant, in the presence of 1nM estradiol, for 24 hours and ERE-luciferase activity assessed. 2-way repeated measures ANOVA with Sidak’s multiple comparisons test, n=3 mean with SD, *P<0.05.

Figure 1

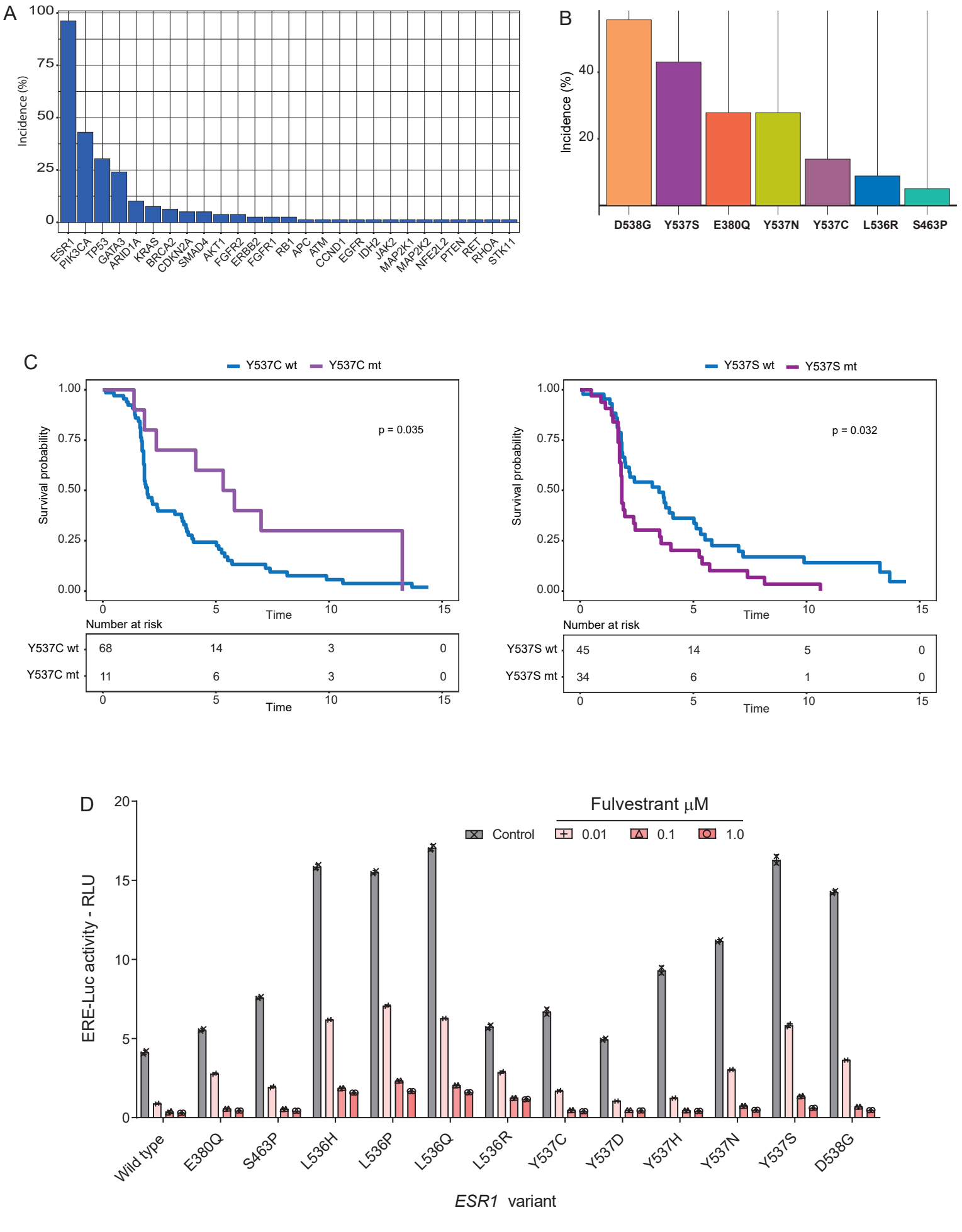
A
Incidence (%)
ESR1
PIK3CA
TP53
GATA3
ARID1A
KRAS
BRCA2
CDKN2A
SMAD4
AKT1
FGFR2
ERBB2
FGFR1
RB1
APC
ATM
CCND1
EGFR
IDH2
JAK2
MAP2K1
MAP2K2
NFE2L2
PTEN
RET
RHOA
STK11
B
Incidence (%)
D538G
Y537S
E380Q
Y537N
Y537C
L536R
S463P
C
Y537C wt
Y537C mt
Survival probability
p = 0.035
Time
Number at risk
Y537C wt 68 14 3 0
Y537C mt 11 6 3 0
Y537S wt
Y537S mt
p = 0.032
Number at risk
Y537S wt 45 14 5 0
Y537S mt 34 6 1 0
D
Fulvestrant μM
Control
0.01
0.1
1.0
ERE-Luc activity - RLU
Wild type
E380Q
S463P
L536H
L536P
L536Q
L536R
Y537C
Y537D
Y537H
Y537N
Y537S
D538G
ESR1 variant

Figure 2

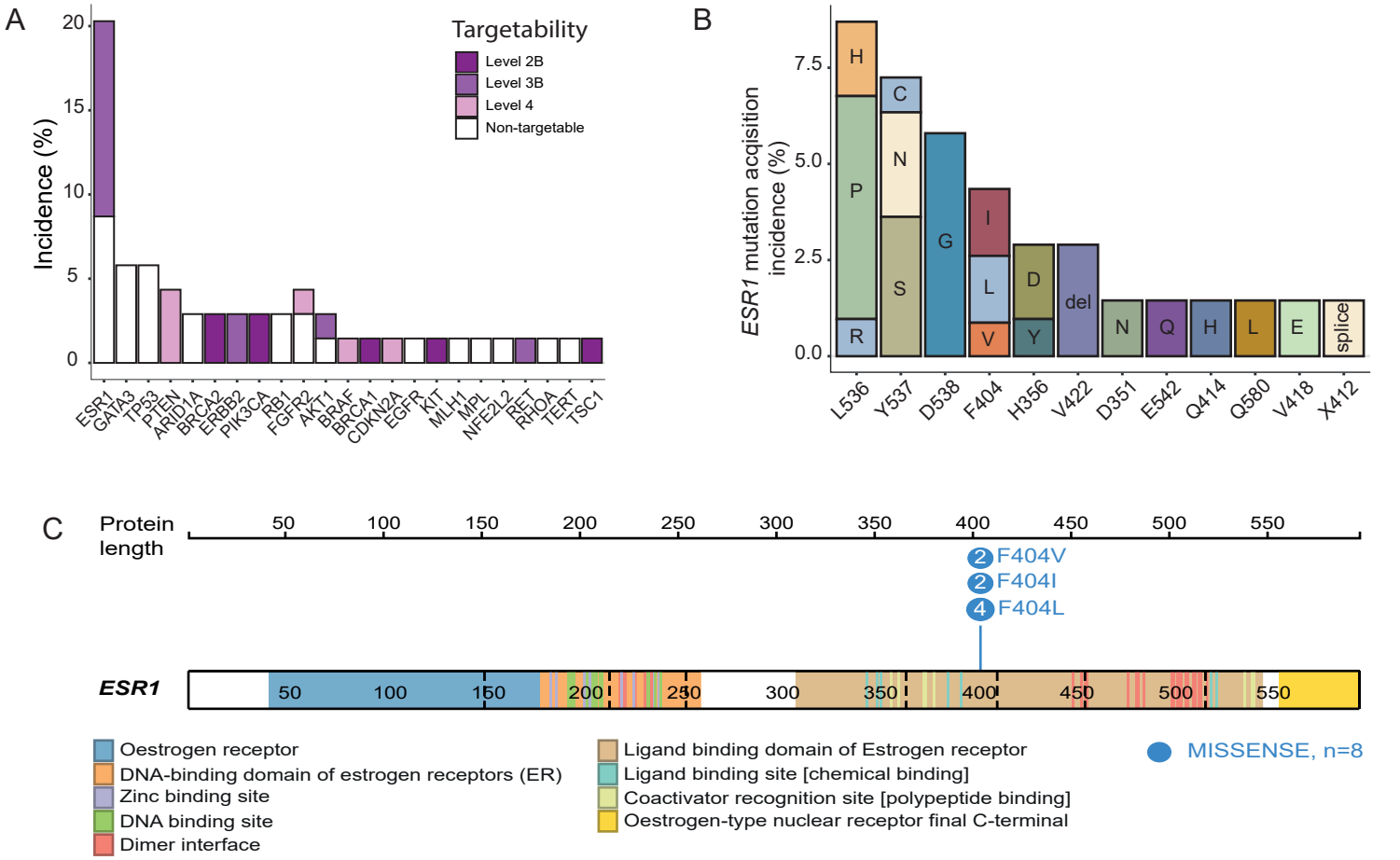
A
Incidence (%)
Targetability
Level 2B
Level 3B
Level 4
Non-targetable
ESR1
GATA3
TP53
PTEN
ARID1A
BRCA2
ERBB2
PIK3CA
RB1
FGFR2
AKT1
BRAF
BRCA1
CDKN2A
EGFR
KIT
MLH1
MPL
NFE2L2
RET
RHOA
TERT
TSC1
B
ESR1 mutation acqisition incidence (%)
L536
Y537
D538
F404
H356
V422
D351
E542
Q414
Q580
V418
X412
C
Protein length
F404V
F404I
F404L
ESR1
Oestrogen receptor
DNA-binding domain of estrogen receptors (ER)
Zinc binding site
DNA binding site
Dimer interface
Ligand binding domain of Estrogen receptor
Ligand binding site [chemical binding]
Coactivator recognition site [polypeptide binding]
Oestrogen-type nuclear receptor final C-terminal
MISSENSE, n=8
D
Patient 1
Patient 2
Patient 3
Clone 1
Clone 2
Clone 3
Clone 4
Clone 5
p.E380Q p.F404I (c.1210T>A)
Cis
p.E380Q
p.F404V (c.1210T>G)
Trans
p.E380Q p.F404I (c.1210T>A)
Cis
p.E380Q p.F404L (c.1210T>C)
Cis
p.E380Q p.F404V (c.1210T>G)
Cis
p.E380Q p.F404L (c.1212T>A)
Cis
p.E380Q p.F404L (c.1212T>G)
Cis
E
Phenylalanine (Phe, F)
Isoleucine (Ile, I)
Valine (Val, V)
Leucine (Leu, L)
F
Estrogen
Fulvestrant

Figure 3

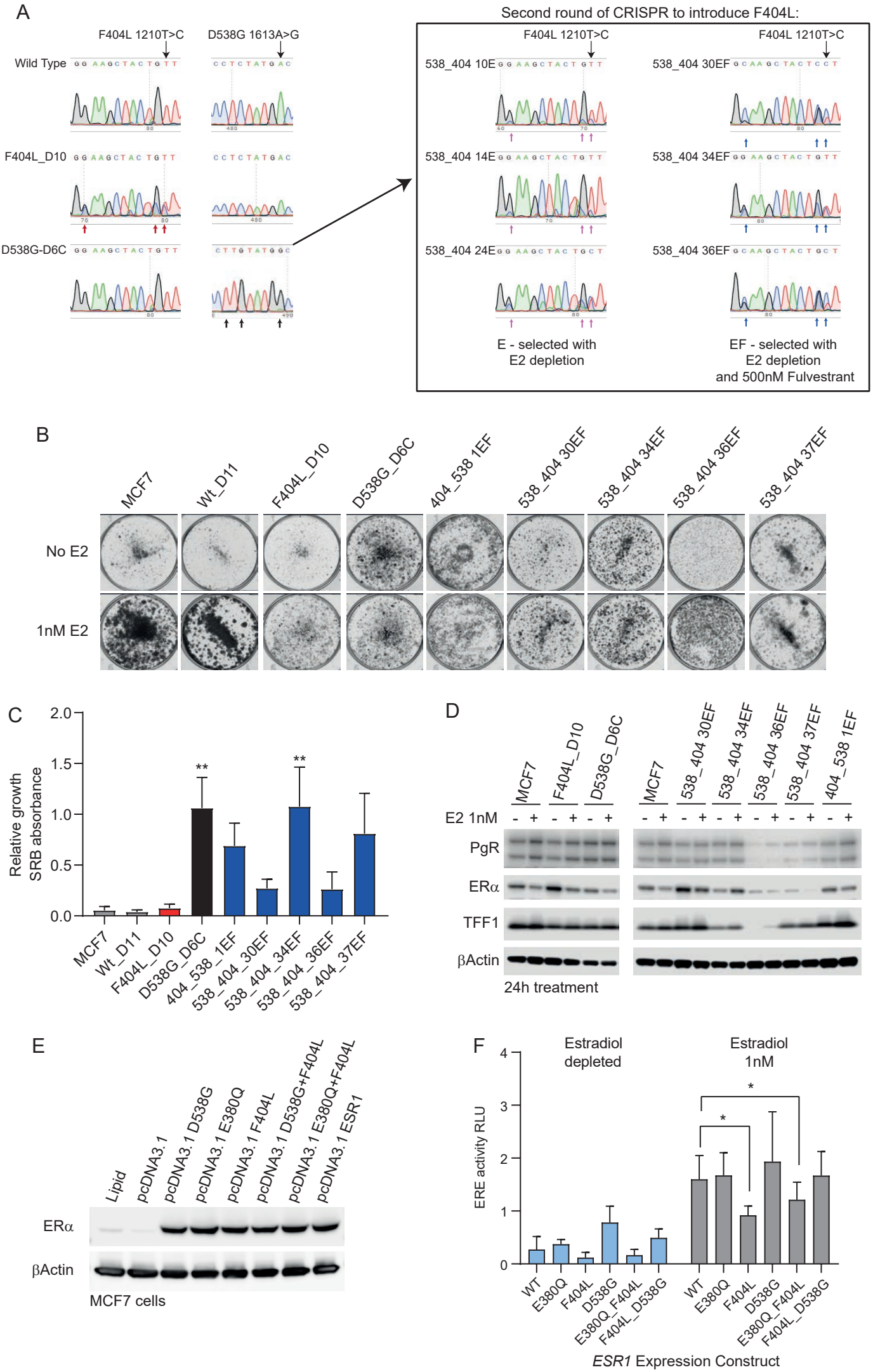
A
F404L 1210T>C
D538G 1613A>G
Wild Type
F404L_D10
D538G-D6C
Second round of CRISPR to introduce F404L:
538_404 10E
538_404 14E
538_404 24E
538_404 30EF
538_404 34EF
538_404 36EF
E - selected with E2 depletion
EF - selected with E2 depletion and 500nM Fulvestrant
B
MCF7
Wt_D11
F404L_D10
D538G_D6C
404_538 1EF
538_404 30EF
538_404 34EF
538_404 36EF
538_404 37EF
No E2
1nM E2
C
Relative growth SRB absorbance
2.0
1.5
1.0
0.5
0.0
**
**
MCF7
Wt_D11
F404L_D10
D538G_D6C
404_538_1EF
538_404_30EF
538_404_34EF
538_404_36EF
538_404_37EF
D
E2 1nM
PgR
ERα
TFF1
βActin
24h treatment
E
Lipid
pcDNA3.1
pcDNA3.1 D538G
pcDNA3.1 E380Q
pcDNA3.1 F404L
pcDNA3.1 D538G+F404L
pcDNA3.1 E380Q+F404L
pcDNA3.1 ESR1
ERα
βActin
MCF7 cells
F
Estradiol depleted
Estradiol 1nM
ERE activity RLU
4
3
2
1
0
*
*
WT
E380Q
F404L
D538G
E380Q_F404L
F404L_D538G
ESR1 Expression Construct

Figure 4

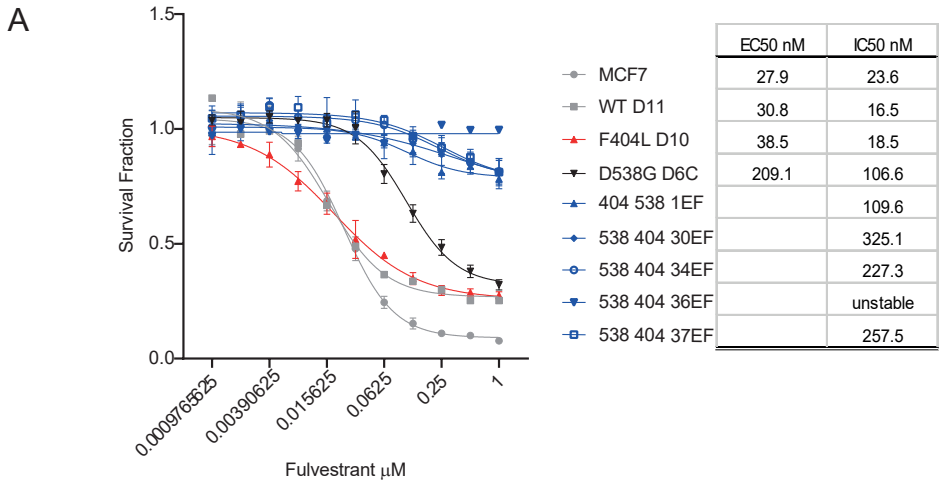

	EC50 nM	IC50 nM
MCF7	27.9	23.6
WT D11	30.8	16.5
F404L D10	38.5	18.5
D538G D6C	209.1	106.6
404 538 1EF		109.6
538 404 30EF		325.1
538 404 34EF		227.3
538 404 36EF		unstable
538 404 37EF		257.5

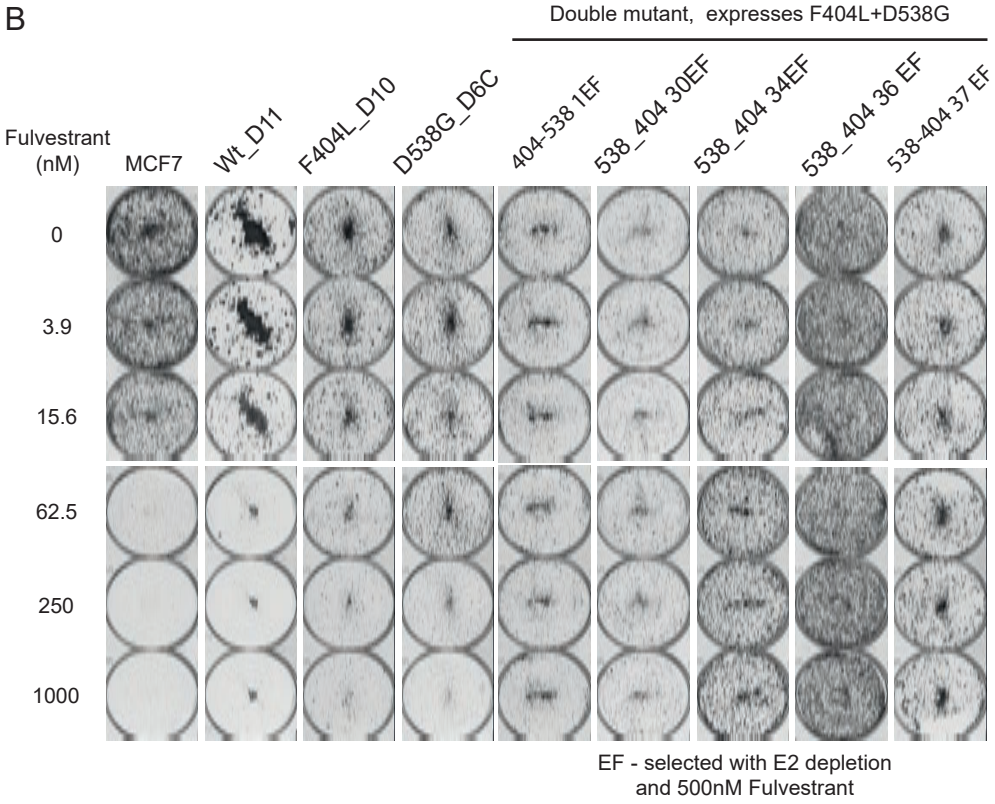

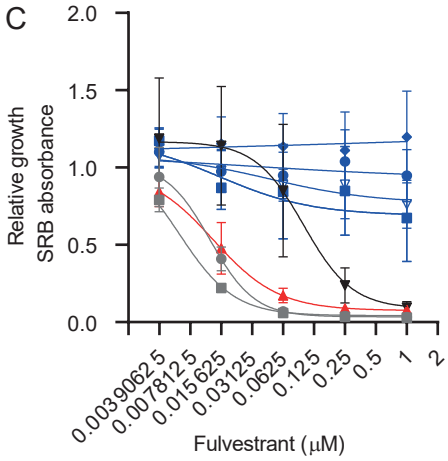

	EC50 nM	IC50 nM
MCF7	12.97	12.14
Wt_D11	7.24	6.177
F404L_D10	14.50	12.98
D538G_D6C	128.92	99.23
404_538_1EF		2.394E+24
538_404_30EF		31.19
538_404_34EF		14.83
538_404_36EF		14.83
538_404_37EF		46.51

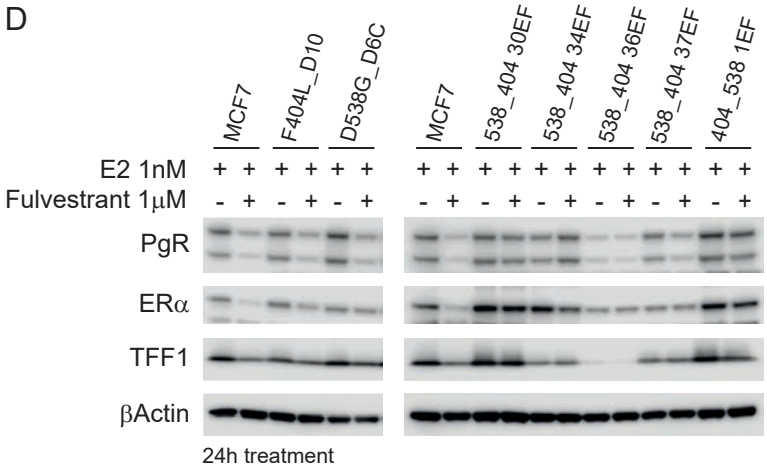

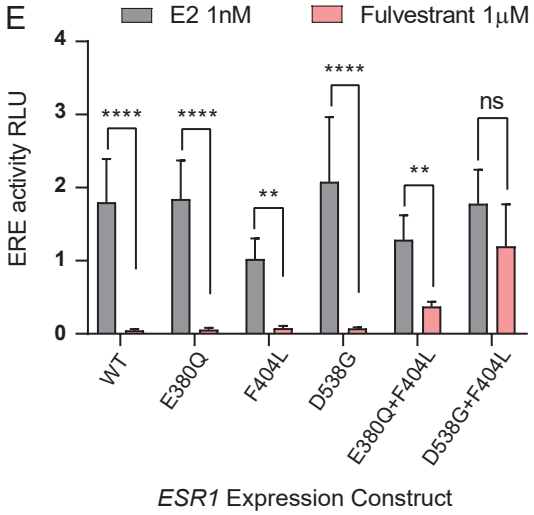

Figure 5

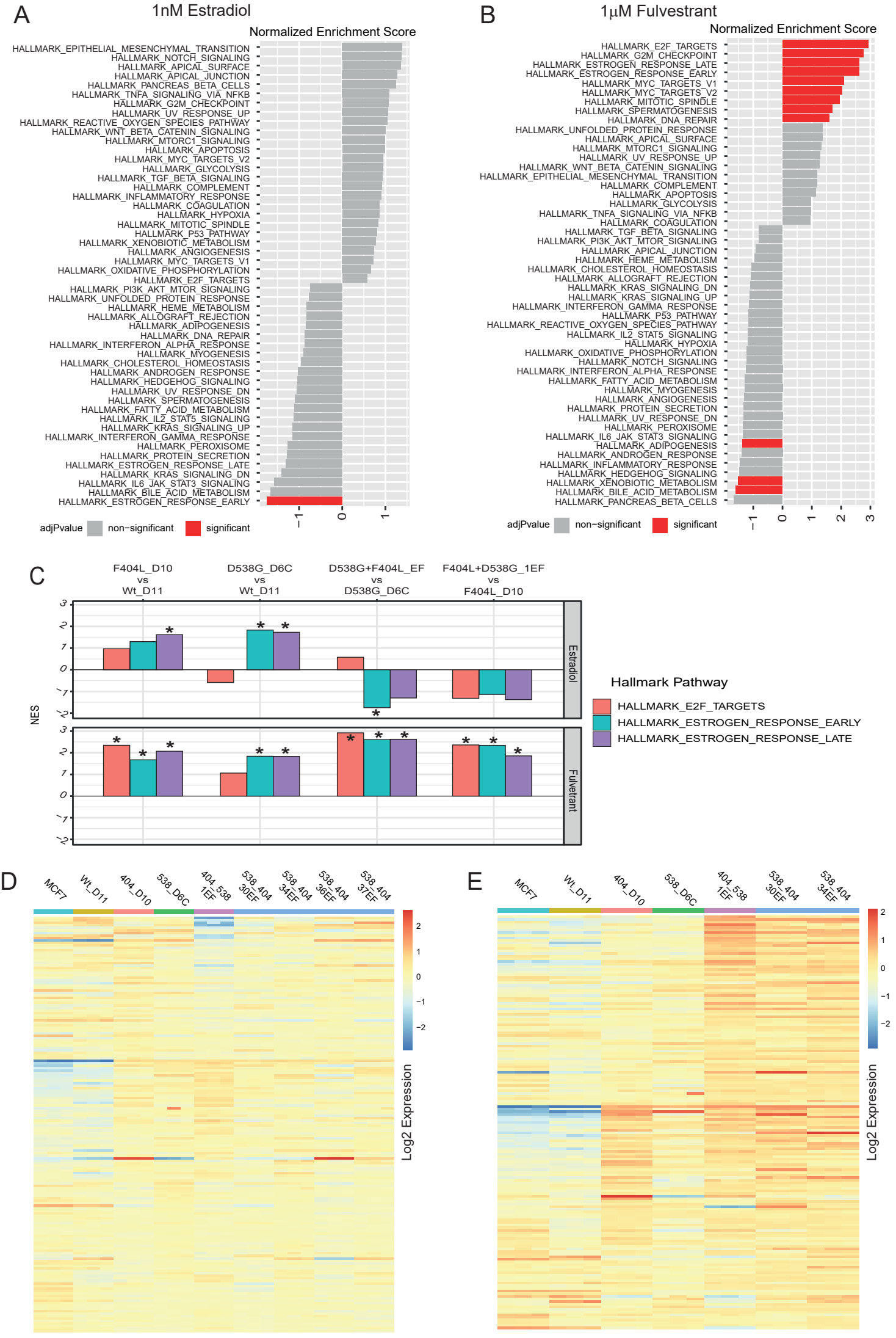
A
1nM Estradiol
Normalized Enrichment Score
HALLMARK_EPITHELIAL_MESENCHYMAL_TRANSITION
HALLMARK_NOTCH_SIGNALING
HALLMARK_APICAL_SURFACE
HALLMARK_APICAL_JUNCTION
HALLMARK_PANCREAS_BETA_CELLS
HALLMARK_TNFA_SIGNALING_VIA_NFKB
HALLMARK_G2M_CHECKPOINT
HALLMARK_UV_RESPONSE_UP
HALLMARK_REACTIVE_OXYGEN_SPECIES_PATHWAY
HALLMARK_WNT_BETA_CATENIN_SIGNALING
HALLMARK_MTORC1_SIGNALING
HALLMARK_APOPTOSIS
HALLMARK_MYC_TARGETS_V2
HALLMARK_GLYCOLYSIS
HALLMARK_TGF_BETA_SIGNALING
HALLMARK_COMPLEMENT
HALLMARK_INFLAMMATORY_RESPONSE
HALLMARK_COAGULATION
HALLMARK_HYPOXIA
HALLMARK_MITOTIC_SPINDLE
HALLMARK_P53_PATHWAY
HALLMARK_XENOBIOTIC_METABOLISM
HALLMARK_ANGIOGENESIS
HALLMARK_MYC_TARGETS_V1
HALLMARK_OXIDATIVE_PHOSPHORYLATION
HALLMARK_E2F_TARGETS
HALLMARK_PI3K_AKT_MTOR_SIGNALING
HALLMARK_UNFOLDED_PROTEIN_RESPONSE
HALLMARK_HEME_METABOLISM
HALLMARK_ALLOGRAFT_REJECTION
HALLMARK_ADIPOGENESIS
HALLMARK_DNA_REPAIR
HALLMARK_INTERFERON_ALPHA_RESPONSE
HALLMARK_MYOGENESIS
HALLMARK_CHOLESTEROL_HOMEOSTASIS
HALLMARK_ANDROGEN_RESPONSE
HALLMARK_HEDGEHOG_SIGNALING
HALLMARK_UV_RESPONSE_DN
HALLMARK_SPERMATOGENESIS
HALLMARK_FATTY_ACID_METABOLISM
HALLMARK_IL2_STAT5_SIGNALING
HALLMARK_KRAS_SIGNALING_UP
HALLMARK_INTERFERON_GAMMA_RESPONSE
HALLMARK_PEROXISOME
HALLMARK_PROTEIN_SECRETION
HALLMARK_ESTROGEN_RESPONSE_LATE
HALLMARK_KRAS_SIGNALING_DN
HALLMARK_IL6_JAK_STAT3_SIGNALING
HALLMARK_BILE_ACID_METABOLISM
HALLMARK_ESTROGEN_RESPONSE_EARLY
−1
0
1
adjPvalue
non−significant
significant
B
1μM Fulvestrant
Normalized Enrichment Score
HALLMARK_E2F_TARGETS
HALLMARK_G2M_CHECKPOINT
HALLMARK_ESTROGEN_RESPONSE_LATE
HALLMARK_ESTROGEN_RESPONSE_EARLY
HALLMARK_MYC_TARGETS_V1
HALLMARK_MYC_TARGETS_V2
HALLMARK_MITOTIC_SPINDLE
HALLMARK_SPERMATOGENESIS
HALLMARK_DNA_REPAIR
HALLMARK_UNFOLDED_PROTEIN_RESPONSE
HALLMARK_APICAL_SURFACE
HALLMARK_MTORC1_SIGNALING
HALLMARK_UV_RESPONSE_UP
HALLMARK_WNT_BETA_CATENIN_SIGNALING
HALLMARK_EPITHELIAL_MESENCHYMAL_TRANSITION
HALLMARK_COMPLEMENT
HALLMARK_APOPTOSIS
HALLMARK_GLYCOLYSIS
HALLMARK_TNFA_SIGNALING_VIA_NFKB
HALLMARK_COAGULATION
HALLMARK_TGF_BETA_SIGNALING
HALLMARK_PI3K_AKT_MTOR_SIGNALING
HALLMARK_APICAL_JUNCTION
HALLMARK_HEME_METABOLISM
HALLMARK_CHOLESTEROL_HOMEOSTASIS
HALLMARK_ALLOGRAFT_REJECTION
HALLMARK_KRAS_SIGNALING_DN
HALLMARK_KRAS_SIGNALING_UP
HALLMARK_INTERFERON_GAMMA_RESPONSE
HALLMARK_P53_PATHWAY
HALLMARK_REACTIVE_OXYGEN_SPECIES_PATHWAY
HALLMARK_IL2_STAT5_SIGNALING
HALLMARK_HYPOXIA
HALLMARK_OXIDATIVE_PHOSPHORYLATION
HALLMARK_NOTCH_SIGNALING
HALLMARK_INTERFERON_ALPHA_RESPONSE
HALLMARK_FATTY_ACID_METABOLISM
HALLMARK_MYOGENESIS
HALLMARK_ANGIOGENESIS
HALLMARK_PROTEIN_SECRETION
HALLMARK_UV_RESPONSE_DN
HALLMARK_PEROXISOME
HALLMARK_IL6_JAK_STAT3_SIGNALING
HALLMARK_ADIPOGENESIS
HALLMARK_ANDROGEN_RESPONSE
HALLMARK_INFLAMMATORY_RESPONSE
HALLMARK_HEDGEHOG_SIGNALING
HALLMARK_XENOBIOTIC_METABOLISM
HALLMARK_BILE_ACID_METABOLISM
HALLMARK_PANCREAS_BETA_CELLS
−1
0
1
2
3
adjPvalue
non−significant
significant
C
F404L_D10 vs Wt_D11
D538G_D6C vs Wt_D11
D538G+F404L_EF vs D538G_D6C
F404L+D538G_1EF vs F404L_D10
NES
Estradiol
Fulvestrant
Hallmark Pathway
HALLMARK_E2F_TARGETS
HALLMARK_ESTROGEN_RESPONSE_EARLY
HALLMARK_ESTROGEN_RESPONSE_LATE
D
MCF7
Wt_D11
404_D10
538_D6C
404_538 1EF
538_404 30EF
538_404 34EF
538_404 36EF
538_404 37EF
Log2 Expression
E
MCF7
Wt_D11
404_D10
538_D6C
404_538 1EF
538_404 30EF
538_404 34EF
Log2 Expression

Figure 6

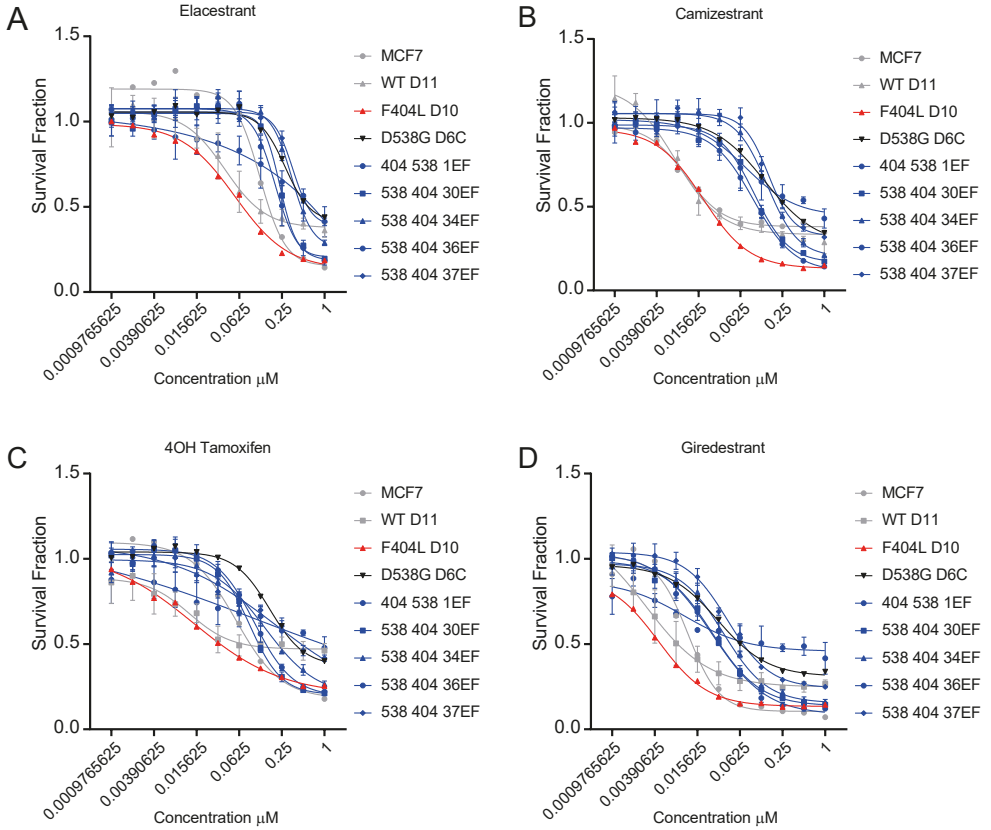
A
Elacestrant
B
Camizestrant
C
4OH Tamoxifen
D
Giredestrant
Survival Fraction
Concentration μM
MCF7
WT D11
F404L D10
D538G D6C
404 538 1EF
538 404 30EF
538 404 34EF
538 404 36EF
538 404 37EF

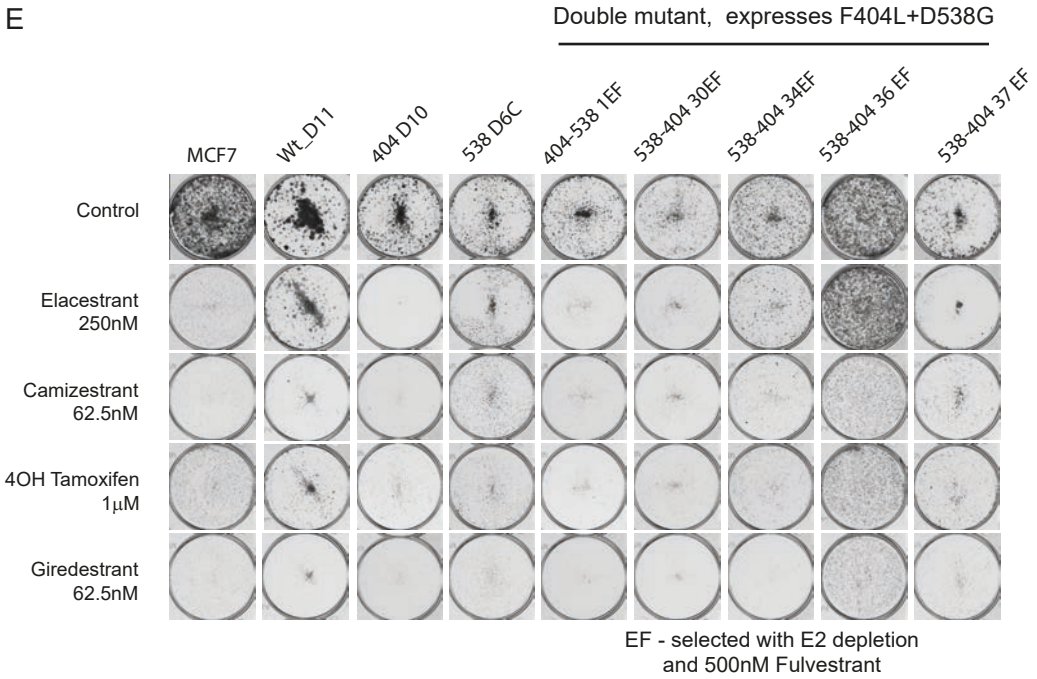
E
Double mutant, expresses F404L+D538G
MCF7
Wt_D11
404 D10
538 D6C
404-538 1EF
538-404 30EF
538-404 34EF
538-404 36 EF
538-404 37 EF
Control
Elacestrant 250nM
Camizestrant 62.5nM
4OH Tamoxifen 1μM
Giredestrant 62.5nM
EF - selected with E2 depletion and 500nM Fulvestrant

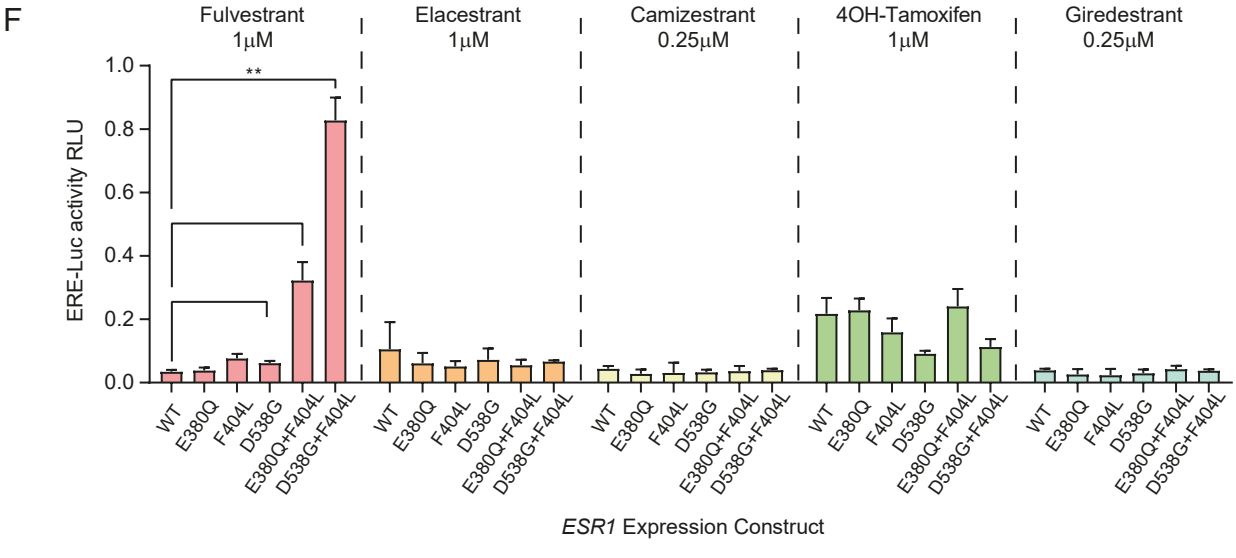
F
Fulvestrant 1μM
Elacestrant 1μM
Camizestrant 0.25μM
4OH-Tamoxifen 1μM
Giredestrant 0.25μM
ERE-Luc activity RLU
**
WT
E380Q
F404L
D538G
E380Q+F404L
D538G+F404L
ESR1 Expression Construct